AFOSR-TR-97

REPORT DOCUMENTATION PAGE

0541

Public reporting burden for this collection of information is estimated to average 1 hour per response, including t gathering and maintaining the data needed, and completing and reviewing the collection of information. Send cd collection of information, including suggestions for reducing this burden, to Washington Headquarters Services, L Davis Highway, Suite 1204, Arlington, VA 22202-4302, and to the Office of Management and Budget, Paperwork Reduction Project (0704-0188), Washington, UC zuous.

1. AGENCY USE ONLY (Leave Blank)	2. REPORT DATE 10/6/97	3. REPORT TYPE AND DATES COVERED Final 9/95 - 9/97

4. TITLE AND SUBTITLE	5. FUNDING NUMBERS
Photochemical and Biological Degradation of Quadracyclane, Dinitramide and Perfluoropolyethers	F49620-44-1-0155 2303/DS 6110 2F 93-N-193

6. AUTHORS
B. Patrick Sullivan, Chemistry, Daniel A. Buttry, Chemistry Patricia J.S. Colberg, Zoology

7. PERFORMING ORGANIZATION NAME(S) AND ADDRESS(ES)	8. PERFORMING ORGANIZATION REPORT NUMBER
University of Wyoming Department of Chemistry and Department of Zoology P.O. Box 3838 Laramie, WY 82071-3838	FQ8671-9400874

9. SPONSORING / MONITORING AGENCY NAME(S) AND ADDRESS(ES)	10. SPONSORING / MONITORING AGENCY REPORT NUMBER
AFOSR 110 Duncan Avenue, Suite B115 Bolling AFB, DC 20332-8080	F49620-94-10155

11. SUPPLEMENTARY NOTES
none

12a. DISTRIBUTION / AVAILABILITY STATEMENT	12b. DISTRIBUTION CODE
unlimited	

13. ABSTRACT *(Maximum 200 words)*

see next page

19971021 251

DTIC QUALITY INSPECTED 4

14. SUBJECT TERMS	15. NUMBER OF PAGES 36
microbiology, photochemistry, dinitramide, quadracyclane	16. PRICE CODE

17. SECURITY CLASSIFICATION OF REPORT	18. SECURITY CLASSIFICATION OF THIS PAGE	19. SECURITY CLASSIFICATION OF ABSTRACT	20. LIMITATION OF ABSTRACT

NSN 7540-01-280-5500

Standard Form 298 (Rev. 2-89)
Prescribed by ANSI Std. Z39-1
298-102

Final Technical Report for "Photochemical and Biological Degradation of Quadracyclane, Dinitramide and Perfluoropolyethers"

Grant Number: 93-NC-193 (PR Number FQ8671-9400874)

Principal Investigator: B. Patrick Sullivan

Co-Principal Investigators : Daniel A. Buttry and Patricia J. S. Colberg

Institution: University of Wyoming

Personnel:

Dr. Norbert Swoboda-Colberg (Postdoc: Colberg)
Song Jin (Graduate Student: Colberg)
Scott Trammell (Graduate Student: Sullivan)
Kevin Seward (Graduate Student: Sullivan)
Yibing Shen (Graduate Student: Sullivan)
Kathy Tomlinson (Graduate Student: Sullivan)
Matthew Monroe (Undergraduate Student: Sullivan)
Rick Cox (Graduate Student: Buttry)
Kevin White (Graduate Student: Buttry)

Abstract: This report describes novel results concerning the chemistry and microbiology of quadracyclane (QC) and dinitramide (DN). No results are presented for perfluoropolyethers, since they were found to be intractable, and therefore resistant to degradation under our experimental conditions.

QC was found to be easily oxidizable at a solid electrode in water to an insoluble, polymeric surface film. The hydrolysis of QC in water yielded two new hydroxy-substituted compounds, in particular, the product tricyclo[2.21.0,6]heptan-3-ol (QCOH) was formed in ca. 90% yield. QCOH is also easily oxidized to give a ketonic product that also yields polymers. Although QC is hydrolyzed on a convenient microbiological timescale to QCOH, the latter has significant biological effects. In active soil microcosms QCOH was depleted from the medium within about 20 days. As it disappeared, a new compound -- a C_7H_8O intermediate -- accumulated in the microcosms. Based on the mass spectra obtained for this compound, it was tentatively identified as either bicyclo[2.2.1]hepta-2-en-5-one or bicyclo[2.2.1]hepta-2,5-dien-5-ol. We have some preliminary evidence to suggest that this intermediate may be subject to further biodegradation in soil under aerobic conditions. Both QC and QCOH were found to be toxic to bacterial cultures, for the former, the LC_{50} values were 0.88 mM and 0.82 mM for *P. aeruginosa* and *P. putida*, respectively. For the latter, the LC_{50} values were 1.2 mM for *P. aeruginosa* and 1.1 mM for *P. putida.*

DN was coaxed to form the first covalent complex, *fac*-Re(bpy)(CO)$_3$N$_3$O$_4$, and its thermal chemistry, spectroscopy and photochemistry were investigated. Its bonding properties were defined, and changes in the infrared spectrum upon coordination were found to be characteristic. It was found that photodecomposition of DN can be sensitized when coordinated to give nitrate, while intermolecular sensitization (by electron transfer) gives nitrite. The latter is in accord with electrochemical studies which point to two, sequential, two electron processes for the reduction of DN to nitrite. Microbiological studies indicated that DN is not used by aerobic bacteria as a sole N source (experiments involved both pure cultures of the genus *Pseudomonas* and aerobic soil microcosms), and is apparently not toxic. In contrast, *P. aeruginosa* is able to catalyze transformation of DN under aerobic conditions, but only when NH_4^+ is present as the N source. The products of DN transformation apparently are NH_4^+ and NO_2^- as is suggested by their increased concentrations in cultures grown in the presence of DN. It is interesting to note that nitrite formation is consistent with a reductive mechanism indicated by our electrochemical studies.

This final report describes our results for the AFOSR funded project "Photochemical and Biological Degradation of Quadracyclane (QC), Dinitramide (DN) and Perfluoropolyethers (PFPE)". Here we present results pertaining to: (1) the redox reactions of quadracyclane in water, (2) the biological degradation of quadracyclane, (3) the reactivity of dinitramide with metals, and the light induced decomposition of DN that is promoted by coordination, (4) the redox chemistry of DN in water, and (5) novel microbiological reactions of DN.

1. Quadracyclane: General Considerations

QC has enjoyed a rich history of investigation that can be traced to its initial discovery in 1936[1]. It has been considered for use as a solar energy storage medium[2], an optical computer memory system[3] and most recently as a high energy aviation fuel.[4] Although extensive studies have been conducted concerning the non-aqueous chemistry of QC and its valence isomerization to norbornadiene,[5-9] very little is known about the chemistry of QC in the event of its release into the environment.[10] The cornerstone in understanding the environmental impact of QC is dissecting the possible reactions of QC in water, in the absence or presence of humic substances or mineral surfaces.

QC (Figure 1) is a seven membered carbon quadricycle containing two cyclopropyl, one cyclobutyl and one cyclopentyl ring. The compound is an indefinitely stable liquid at room temperature with a modest vapor pressure under normal conditions (b.p. 108 C @740 mm Hg). The strain energy due to ring size and the rigid molecular conformation of the molecule is approximately 81 Kcal/mol.[11]

The unusual reactivity of QC is due to ring strain, and generally results in the cleavage of the C2-C6 cyclopropyl bond. In addition, QC readily undergoes photochemically,[12] electrochemically[20] and chemically[13] initiated conversion[15] to its lower energy valence isomer, norbornadiene (NB), hence representing an important concern in understanding the overall chemistry of the molecule. A detailed description of the investigated chemistry and appropriate the

1

references for further reading can be found in bibliography notes 10 to 15. The scope of this report will be limited to the aqueous chemistry of QC, which has a special relevance for environmental concerns.
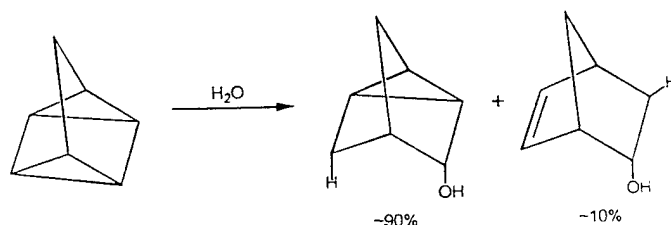

Figure 1. Hydrolysis of Quadracyclane to alcohol products

Prior studies by Sullivan *et. al.*[16] at the University of Wyoming concerned with the synthesis of QC hydrolysis products found that QC undergoes hydrolysis at the C1-C6 bond to form a simple mixture of products (Figure 1), a tricyclic alcohol, tricyclo[2.21.0,6]heptan-3-ol (**QCOH**), and a bicyclic alcohol, bicyclo[2.2.1]hepta-5-en-2-ol. The hydrolysis reaction is very fast on an environmental time scale. In under an hour at standard conditions, a saturated aqueous solution (1.4 mM in QC) of QC begins conversion to its hydroxylated forms and after 2-3 days a conversion of >80% is realized. Experiments conducted by ^{13}C NMR spectroscopy (White and Buttry[17]) confirmed the above results, and verified the product ratios.

Extensive electrochemical studies have been conducted concerning the reductive[18] and oxidative[19] chemistry of QC in non-aqueous environments. The most outstanding of the findings by these investigations is the amazingly low anodic oxidation potential for QC relative to other formally saturated hydrocarbons. At 0.91 V vs. SCE in acetonitrile solution the oxidation potential for QC is substantially lower than the values of 2.0-2.5 V vs. SCE exhibited by alkyl substituted cyclopropanes.[20] The electrochemical oxidation of QC also was reported to cause the production of what was referred to as a "fouling film" on the electrode,[14,21] which caused passivation of the electrode and necessitated its mechanical removal from the surface. Speculation as to the

2

composition and formation pathway of this robust surface film was never attempted and is the subject of one of the investigations of this report.

Several well established analytical techniques have been enlisted in our investigations and will be mentioned and referenced in order to provide the reader with the opportunity to further study their intricacies. Although the reactions of QC and its analogs are relatively fast on an environmental time scale, they are slow and therefore relatively impractical on the laboratory time scale. Various electrochemical methods were chosen and implemented for their innate ability to provide, in a controlled fashion, the driving force for, and an accurate account of, the occurrences in the various chemical reactions. All of the applied electrochemical techniques are well described in reference 23. Nuclear magnetic resonance spectroscopy (NMR) and Fourier transform infrared spectroscopy (FTIR) were used to characterize the starting materials and the reaction products of the electrochemical experiments. The development of theory for these two techniques is so well established that one can find a thorough discussion in any general organic chemistry text. In addition to the traditional transmission infrared spectroscopic techniques, a method known as attenuated total reflectance spectroscopy (ATR-FTIR) was used. The technique allows for the direct probing of surface moieties by infrared spectroscopy and was used extensively in the characterization of the aforementioned fouling film. A full description of the ATR technique can be found in reference 24.

1.1. Electrochemical Oxidation of QC. Figure 2 Shows the cyclic voltametric response of QC at a gold electrode in an aqueous environment. Upon comparison to the background (inset) it is obvious that QC undergoes an anodic oxidation in water. Based on the fact that the E_p for the major anodic feature is at 0.80 V, 0.10 V lower than the reported non-aqueous standard potential,[19] it seems that the oxidation is even slightly more facile in water. The more interesting of the two features is the pre-wave that has an E_p value at ~0.20 V, which is roughly 1.5 V lower in potential than comparable unstrained hydrocarbons. Electrochemical oxidation in this manner formed the characteristic fouling film on the electrode surface which was further investigated with ATR spectroscopy.
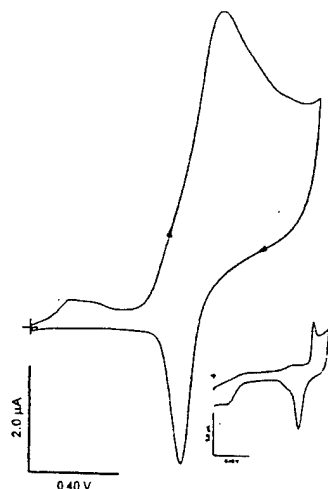
**Figure 2.** CV of an aqueous solution of QC on a gold electrode.

A technique developed by White and Buttry[17] was used to coat a gold foil electrode with the QC oxidation product at three potentials between 0.0 and 0.85 volts which were examined by ATR-FTIR to determine if there were differing compositions in the films. Rather than repeating the scanning process until the potential decay due to the film formation was observed the electrode was scanned only once to give a true idea as to the extent of oxidation occurring at the bare gold surface. The three potentials were: 0.20 V, the E_p for the pre-wave, 0.40 V, at the base of the major oxidation feature, and 0.85 V, which is slightly more positive than the E_p for the major feature. Upon examination by IR spectroscopy it was evident that the spectral features were the same for all the films produced indicating that oxidation of QC was actually occurring at the pre-wave potential. The only differences were the intensities of the signals which also gave insight into the nature of the electrode process.

The IR signal intensities of the films produced at the first two potentials (0.02 and 0.40 V) were essentially identical with the latter being only slightly more intense. The signal of the final film, produced at 0.85 V, showed an intensity that was higher than the former two films. These findings suggest that at the lower potential, on bare gold, the oxidation of QC to its final product occurs and this material is deposited in some fashion on the electrode surface. No further oxidation occurs until sufficiently positive potentials are reached at which time oxidation of the bulk QC in

4

solution occurs and deposits a thicker film on the surface which is interpreted as a more intense IR signal.

A rotating disc electrode electrochemical technique developed by White and Buttry[17] to circumvent complications to the theoretical treatment of the data by the formation of the fouling film were implemented to give insight into the number of electrons transfered in the rate limiting step of the electrochemical reaction. After treatment of the data it was found that the rate limiting step of the QC oxidation was a multi-electron process.[18]

Assimilation of the data provided by the electrochemistry experiments, the infrared spectroscopy, and previous work by Wright,[22] lead to the proposal of a possible polymerization mechanism for the formation of the fouling film. In Scheme 1, QC undergoes the expected one electron oxidation to the QC$^+$, which rapidly converts to the norbornadiene cation radical. Loss of H$^+$ and addition of water generates the hydroxylated NB, which is further oxidized by two electrons to the NB ketone radical. Upon radical coupling, a dimer is formed that is similar to a species reported by Wright[22] which showed a fast auto polymerization to an unknown polymer.
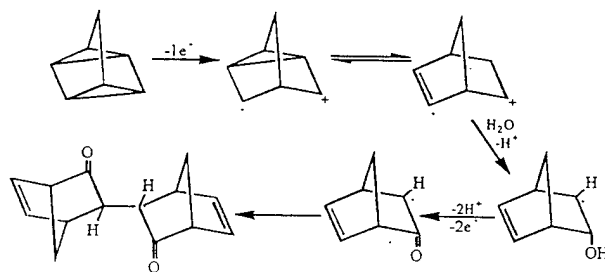
Scheme 1. Proposed mechanism for the formation of a QC-derived reactive dimer under oxidizing aqueous conditions.

Scheme 2 is the proposed radical pathway for the QC oxidation dimer polymerization. The dimer radical is generated by its reaction with one of the electrochemically formed monomeric

5

radicals. Radical coupling occurs and propagation is terminated when the polymer layer becomes too thick and no more QC^+ can be formed at the electrode.
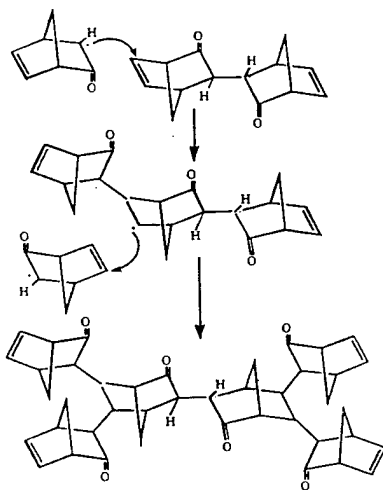
Scheme 2. Proposed mechanism for QC polymerization.

1.2. Redox Reactions of Tricyclo[2.21.0,6]heptan-3-ol (QCOH).

Similar experiments were performed on quadricyclane's hydroxylated form (QCOH) in order to better understand its fate in the environment. The cyclic voltammetry of QCOH was not as information-rich as that for its parent compound, but it did reveal that like QC, QCOH has an unusually low oxidation potential and forms a fouling film on the electrode surface. The film was investigated with ATR which revealed a diversity of products that proved impossible to dissect without further information from differing techniques. The spectra did indicate the oxidation of the OH of QCOH to the expected ketone and the opening of the ring structure to some straight chain hydrocarbon moiety.

In an attempt to generate enough oxidized QCOH which was did adhere to the gold substrate, and in order to facilitate the use of NMR spectroscopy for characterization of the resulting compounds, QCOH was subjected to bulk oxidations by iron(III) nitrate and cerium(IV) ammonium sulfate dihydrate.

6

In the case of the Ce salt, reaction of one equivalent of metal with one equivalent of QCOH brought about no noticeable change in the IR spectrum of the product as compared to the parent compound. Upon reaction with two equivalents of the Ce salt the product spectrum showed the presence of an FTIR band characteristic of a ketone stretch indicating the oxidation of the -OH group to the corresponding ketone. Reaction of QCOH with four equivalents of the Ce salt decreased the intensity of the frequency associated with the cyclopropyl ring C-H stretching and intensified and added shoulders to the ketone band. This indicates that further reaction with the Ce salt opens the cyclopropyl ring, and incorporates additional oxygen into the system (from the aqueous solvent) which is oxidized to a ketone.

The results of the Fe salt oxidations were not as easily defined as the corresponding Ce oxidations. Reaction of one equivalent of Fe(III) with one equivalent of QCOH elicited a product that defied accurate assessment of composition. A decrease in OH stretching intensity was accompanied by the increase in intensity of a band that is in the ketone range but was unexplainably low for the type of compound expected for the reaction. Further oxidation by two and then four equivalents of Fe(III) showed and increase in the aforementioned band, decrease in the C-H cyclopropyl stretch and the growth of a band more characteristic of the expected ketone stretch. Clearly there is complex chemistry occurring between the iron and QCOH but it is difficult at best to describe it with the techniques applied in this study.

1.3. Conclusions: Redox Reactions of QC and QCOH. The highly strained nature of the compound, which makes it such an attractive candidate for a high energy fuel, tends to complicate the aqueous chemistry of the compound. The tendency of QCOH to readily form from QC may pose serious large quantity storage problems especially in humid climates. QCOH itself is oxidized at low potentials to yield further oxygenated products. One must also consider the relatively low barrier that stands between QC and the formation of its polymeric form in the presence of water. It could be conceived that the fouling of fuel delivery systems and the coating of storage vessels by the robust polymeric film could pose a potentially dangerous problem.

2. Microbiological Degradation of Quadracyclane: General Considerations.

As mentioned above, our first results demonstrated that the hydrolysis of quadracyclane (QC) to two alcohols, tricyclo[2.21.0,6]heptan-3-ol (QCOH or tricyclic alcohol), and bicyclo[2.2.1]hepta-5-en-2-ol (bicyclic alcohol) occurs in distilled water over long periods of time. We have also found that the reaction is promoted by light, especially in the presence of colloidal hematite. The hydrolysis reaction is of great significance and must be taken into account when examining the microbiological degradation of QC

As a prelude to our microbiological studies, the hydrolysis reaction was examined under culture conditions. It was found that quadracyclane disappeared completely within five days when incubated in 100 mM phosphate buffer (at its solubility limit), while quadracyclane concentrations in sterile distilled water remained almost unchanged over the same analysis period.

During quadracyclane depletion both tricyclic and bicyclic alcohol were detected by GC/MSD analysis. Their identities were confirmed by comparison with a authentic samples of bicyclo[2.2.1]hepta-5-en-2-ol (Aldrich) and tricyclo[2.2.1.0^{2,6}]heptan-3-ol. Formation of these two compounds is in agreement with recent findings of other investigators in pure water under thermal and photochemical conditions, and were the only products formed under these experimental conditions. Greater than 80% of the quadracyclane is converted to the tricyclic-alcohol within five days; the balance is converted to the bicyclic-alcohol degradation product. These alcohol derivatives of quadracyclane are one to two orders of magnitude more soluble in water than the parent compound, which is certainly of significance for environmental transport.

The rate and extent of abiotic quadracyclane transformation apparently increases with increasing ionic strength. This is suggested by quadracyclane measurements made in serum bottles containing sterile distilled water or sterile phosphate buffer at two different concentrations (10 mM and 100 mM). In these experiments, quadracyclane incubated in 100 mM phosphate buffer is completely converted to the cyclic alcohol derivatives within five days, while 45% of the parent compound is converted to degradation products in 10 mM phosphate buffered solution.

8

2.1. Soil Microbe Transformations of tricyclo[2.2.1.0^{2,6}]heptan-3-ol.

Since quadracyclane itself is converted to alcohols abiotically, and is apparently unreactive by itself to soil microbes, we studied the major degradation product tricyclic[2.2.1.0^{2,6}]heptan-3-ol. Thus, a purified sample of tricyclic-alcohol was used in conjunction with soils from an uncontaminated local garden. Soil microcosms were established in 165-mL sterilized serum bottles with soil: minimal salt media = 1g:10 mL. The medium consisted of the following: 28 mM KH_2PO_4, 72 mM K_2HPO_4, 8 mM $(KH_2)_3PO_4$, 0.3 mM $MgSO_4$, 30 μM NaCl, 7 μM $FeSO_4 \cdot H_2O$, 12 μM $MnSO_4$, 14 μM $CaCl_2$, pH at 7.1. Autoclaved microcosms amended with 1% formaldehyde served as abiotic controls. All serum bottles were incubated in the dark at room temperature. Tricyclic-alcohol, bicyclic-alcohol and other possible products were monitored by GC as described previously.

Under these conditions we have established that tricyclic-alcohol is persistent for several months in the control microcosms. Chemical transformation apparently did not occur. In active soil microcosms, however, tricyclic-alcohol was depleted from the medium within about 20 days As the tricyclic derivative disappeared, a new compound -- a C_7H_8O intermediate -- accumulated in the microcosms. Based on the mass spectra obtained for this compound, it was tentatively identified as either bicyclo[2.2.1]hepta-2-en-5-one or bicyclo[2.2.1]hepta-2,5-dien-5-ol. We have some preliminary evidence to suggest that this as yet unidentified intermediate may be subject to further biodegradation in soil under aerobic conditions. The new bicyclic derivative is apparently persistent in soil; however, the absence of soil microorganisms that are able to further metabolize such compounds may account for its observed recalcitrance.

Lacking isolates of microbial strains that can use tricyclic-alcohol as a sole source of carbon, typical growth-linked mineralization could not be confirmed by direct cell counts or other biomass measurements. In other studies using the biometer flask technique, however, we have observed enhanced carbon dioxide production in the active soil microcosms amended with tricyclic-alcohol than in soils which were not amended with the tricyclic derivative. In addition, when tricyclic-alcohol was exposed to the active soil microcosms, it was depleted at much faster

rate than in the initial experiments. These observations are consistent with the phenomenon of enhanced biodegradation found when certain compounds are exposed to microorganisms continuously.

2.2 Bacterial Studies of Quadracyclane and tricyclo[2.2.1.0^{2,6}]heptan-3-ol.

Since tricyclic-alcohol is a dominant abiotic product of quadracyclane degradation and is probably capable of being converting into the bicyclic-alcohol, we chose the former as the compound of interest in a second study involving a common bacterial genus, *Pseudomonas*. In addition, we have used hydrocarbon contaminated soils in the expectation that hydrocarbon degrading microorganisms will also act upon quadracyclane or tricyclic-alcohol The objectives of this study were to: (1) evaluate the persistence of tricyclic-alcohol in a soil environment; (2) evaluate potential growth inhibition of tricyclic-alcohol on two representative hydrocarbon-degrading soil bacteria, *Pseudomonas aeruginosa* (ATCC 15526) and *P. putida* (ATCC 12633); (3) determine the acute toxicity of tricyclic-alcohol on the two bacteria and obtain the 50% lethal concentration (LC$_{50}$) of tricyclic-alcohol; and (4) assess the potential toxicity of tricyclic-alcohol on microbial activity in soils using most probable bacterial number (MPN) measurements and respiration in biometer flasks. Here, we report the persistence of quadracyclane-transformed tricyclic-alcohol. We also address the toxicity of quadracyclane and tricyclic-alcohol on pure cultures of *Pseudomonas* and on soil bacteria.

In soil microcosm studies, we used gasoline-contaminated soil to maximize the probability of quadracyclane degrading bacteria being present, because quadracyclane-contaminated soils were not available. Gas chromatographic analyses suggest that quadracyclane is transformed into the two alcohols within 5 days, and although quadracyclane disappeared rapidly in 5 days, both alcohols were persistent in the soil microcosms for several weeks.

In pure culture studies, *Pseudomonas aureginosa* and *P. putida* were grown in LB medium. Various concentrations of tricyclic-alcohol were added to the media. The controls in these cases had typical exponential growth curves. However with increasing concentrations of tricyclic-alcohol in all treatments, the growth curve sloped down, suggesting the growth rate

10

decreased. The inhibitory effects increased with increasing tricyclic-alcohol concentration, except for 2 mM and 6 mM, where a saturation effect was observed . The 50% growth inhibition concentrations at 48 hr incubation for the two strains were determined to be 0.68 mM for *P. aeruginosa* and 0.48 mM for *P. putida* using "TOXSTAT" software.

In autoclaved deionized water and in minimal salts solution, the LC_{50} for the two *Pseudomonas* strains exposed to varying concentrations of pure quadracyclane and tricyclic-alcohol were measured after 48 hr of incubation. In the quadracyclane test, the LC_{50} values were 0.88 mM and 0.82 mM for *P. aeruginosa* and *P. putida*, respectively. In the tricyclic-alcohol test, the LC_{50} values were 1.2 mM for *P. aeruginosa* and 1.1 mM for *P. putida*.

A biometer flask system was used for the determination of total soil respiration during exposure to tricyclic-alcohol. Uncontaminated garden soil was used as the sample source. Total soil respiration (TSR) did not change significantly following treatment with tricyclic-alcohol, although there were some differences between the control and experimental treatments at the beginning of the experiments. TSR decreased with increased concentration of tricyclic-alcohol added. Most probable number measurements were made in biometer flasks at initial setup and following 3 days of incubation. In that period, bacterial population numbers dropped from 6×10^6 cells/mL in the controls to 2.1×10^5 cells/mL in 6 mM treatments.

2.3. Significance of the Results.   Hydrocarbons, including petroleum hydrocarbons, are usually susceptible to biological transformation or degradation.[25-27] Quadracyclane was found in our studies to be quickly transformed into alcohol products. This stands in contrast to the reported isomerization reactions that produce 2,5-norbornadiene in the presence of light or metals.[28-30] In addition to the chemical transformation, quadracyclane is also photolyzed to the alcohol products when exposed to UV light as we demonstrated in the first year report. From this data It is quite safe to conclude that quadracyclane exists in the forms of tricyclic- and bicyclic-alcohols in the natural environment, and only in deionized water in the dark is quadracyclane relatively stable.

In the soil microcosm studies, tricyclic-alcohol was found to be persistent in gasoline-contaminated soils for months when at a concentration of 0.8 mM, even under aerobic conditions, which is usually favorable for hydrocarbon biodegradation.[31] This is an unexpected result, because alcohol derivatives usually are very susceptible to microbial degradation and mostly serve as metabolic intermediates in microbial biodegradation.[31,32] Usually such alcohols are eventually broken down to final products such as CO_2 and H_2O. The recalcitrance of tricyclic-alcohol to active soil microbial degradation implies the potential for tricyclic-alcohol to be hazardous to soil microorganisms. In the meantime, other abundant carbon sources in the gasoline-contaminated soils could be preferred as energy sources, and the biodegradation of quadracyclane is deterred because soil micoorganisms are not adapted to it.

As described above, we used two *Pseudomonas* strains, *P. aeruginosa* and *P. putida*, as experimental organisms to test the acute toxicity of quadracyclane and tricyclic-alcohol. The choice of the two *Pseudomonas* strains was based on their widespread occurrence in soils and their documented ability to perform hydrocarbon degradation. Growth of the two microbes was observed to be inhibited by tricyclic-alcohol; the inhibitory effect was enhanced with increased concentration. The inhibitory mechanism is not clear, we assume that the tricyclic-alcohol acts in a manner similar to organic solvents, which directly affect the cell membrane components and permeability.

In a further toxicity study, LC_{50} was measured. Bacteria cells were exposed to quadracyclane in distilled water for a short time to obtain the quadracyclane LC_{50}. The LC_{50} for tricyclic-alcohol was tested in phosphate buffered saline solution. LC_{50} values suggest similar toxicities for the two compounds. At about 1 mM concentration, toxicity of quadracyclane and tricyclic-alcohol are significant.

In natural soils, tricyclic-alcohol is a major form in which quadracyclane exists. To determine the toxicity of tricyclic-alcohol to general soil microorganisms, garden soils were established in microcosms. Tricyclic-alcohol toxicity was measured based on the cell population density changes. In a 3-day test, cell population density dropped significantly with increased

concentration of tricyclic-alcohol. These findings show that the acute toxicity of tricyclic-alcohol to general soil microorganisms. However, in the biometer flask studies, TSR was not dramatically affected by tricyclic-alcohol in a long run. This could be explained by two hypotheses: (1) tricyclic-alcohol was adsorbed to soil particulates and, therefore, its actual effective concentration was eliminated; and (2) some strains of soil microbes could adapt to tricyclic-alcohol after a period of exposure and use tricyclic-alcohol as a carbon source for cellular metabolism. The input of tricyclic-alcohol served as an extra energy source, especially when tricyclic-alcohol is at low concentration such as 0.5 mM. The metabolism of those organisms which could use tricyclic-alcohol increased and probably compensated for the loss of other microbial respiration due to tricyclic-alcohol toxicity.

The results of these preliminary toxicity studies of tricyclic-alcohol and quadracyclane provide some useful information for future experimentation with these compounds, as well as highlighting the need for concern regarding their storage and disposal. The potential for biodegradation, however, points to the need for further research on the microorganisms which are capable of metabolizing quadracyclane and tricyclic-alcohol.

3. Dinitramide: General Considerations

The dinitramide ion, $N_3O_4^-$, is a relatively new member of the large class of nitrogen oxyanions. Although, it has found application as a solid propellant, its chemistry, especially involving metal complexation and redox properties is poorly developed. Preparation and spectroscopic characterization of the complexation modes of $N_3O_4^-$ could be key in understanding its adsorption behavior on naturally-occurring mineral surfaces which in turn could play a role in the environmental transport and fate of water soluble salts. Characterization of its redox properties will help to understand reactions with naturally-occurring oxidants and reductants. No biological results have been reported previously.

3.1. Structure and Bonding Considerations.

An understanding of the reactivity and bonding propensity of $N_3O_4^-$ can be gleaned by consideration of the eight fundamental resonance structures shown in Figure 5.[33]
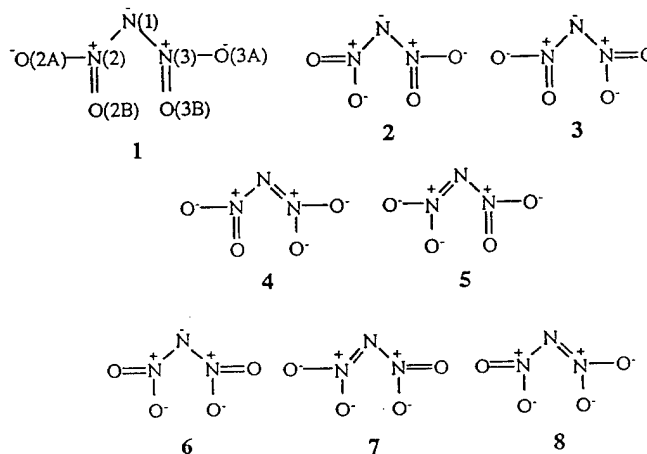

Figure 5. Fundamental resonance forms of DN.

Resonance forms 1-3 would likely make the most substantial contribution to the total electronic structure since the negative charges on oxygen are well separated. By the same argument, 6-8 would not likely make any significant contribution since adjacent negative oxygen atoms would be unstable.[34] Calculated atomic charges (RHF/6-31*6) agree with this picture of delocalization since large and nearly equal negative charges on the oxygen atoms and a negative charge on the central nitrogen atom would be expected, N1 (-0.306), N2 and N3 (+0.729), O2A and O3A (-0.545) and, O2B and O3B (-0.531).[35] In this picture, the net negative charge is delocalized over the molecule which results in strengthening of the N-NO$_2$ bonds.[36] In fact, the dinitramide ion is more stable with respect to alkyl dinitramines and nitramide in terms of its acid-base sensitivity, thermal, and shock stability.[37,38]

Although the resonance forms in Figure 5 are instructive, they do not indicate the conformational disposition of the ion. However, *Ab initio* calculations at the MP2 level using a 6-31G** basis set show that the minimum-energy structure has C_2 symmetry in which the oxygen

14

atoms are above and below the plane of the three nitrogen atoms.[35] A non-local density functional study using the Gaussian DZVPP basis set gives similar results.[34]

Despite packing effects that take place in a single crystal, the calculated results are in good agreement with the structural data obtained from crystallographic results of several dinitramide salts[39] The rotation of the nitro-groups out of the N-N-N plane has been rationalized in two different fashions. The first, and simplest, is that oxygen atoms in close proximity are trying to increase their separation by rotating away from each other.[34] The second idea employs the use of the two lone pairs on the central nitrogen atom. Thus, in a bonding interaction, assuming the distribution of the electron pairs around the central nitrogen atom is close to tetrahedral (which is supported by the N-N-N angles of ca. 112°), a rotation of the nitro-groups by 27° would give their π electrons maximum overlap with the lone pair orbitals on the central nitrogen, thus optimizing conjugation.[34]

From the electronic and geometric structural considerations, it is clear that several modes of binding to transition metals are possible. For monodentate coordination either N or O bound modes can occur, with the O bound form being most likely for hard, electropositive metal ions and the N-bound form (involving the central skeletal nitrogen) most likely for softer metal ions. So far, very few studies of dinitramide-metal ion reactions have been published. X-ray crystallographic results from hydrated dinitramide metal salts of Mn^{2+} and Zn^{2+} show the cations coordinated by water with the dinitramide anion outside the coordination sphere.[40] Hydrated dinitramide salts of Cu^{2+}, Ni^{2+}, Co^{2+}, Fe^{2+} and Ag^+ show similar IR $N_3O_4^-$ modes as for KN_3O_4 and are reported to have no covalent bonding.[41] A brief paper reported the covalent compound $Hg(N_3O_4)_2$, but the nature of the bonding was not specified.[42] In polar solvents the compound ionizes to Hg^{2+} and $N_3O_4^-$, however, in non-polar media the covalent structure is still apparently intact. N or O bonded covalent structures are possibilities and with the results of IR and UV-vis studies, an O bonded structure was proposed. For example, the structure of $Hg(N_3O_4)_2$ was not assigned as N bonded since its UV-vis spectra in non-polar solvents did not coincide with

the known UV-vis spectra of $HN(NO_2)_2$. From IR studies, an O bond structure was proposed since IR spectra of an O-alkyl ether of the *aci*-dinitramide and $Hg(N_3O_4)_2$ were similar.[42]

Our work has resulted in the preparation of the first unequivocally covalent metal-dinitramide complex, *fac*-Re(bpy)(CO)$_3$N$_3$O$_4$, and its thermal chemistry, spectroscopy and photochemistry. Use of a third row transition metal as a probe of bonding is dictated by the stability of the metal ligand bond. As will be discussed, by comparison with the properties of other Re complexes including the nitro complex, *fac*-Re(bpy)(CO)$_3$NO$_2$, we can conclude that the N-bound dinitramde ligand is a weak net σ-donor and a weak net π-acceptor.

3.2. Preparation and X-Ray Crystal Structure of *fac*-Re(bpy)(CO)$_3$N$_3$O$_4$. The preparation of the first demonstrated coordination complex of the dinitramide ion was accomplished by reaction of KN$_3$O$_4$ with the reactive precursor *fac*-Re(bpy)(CO)$_3$OSO$_2$CF$_3$ at room temperature in water. Slow recrystallization of the yellow solid from this reaction using a hexanes/CH$_2$Cl$_2$ mixture afforded thin yellow plates of *fac*-Re(bpy)(CO)$_3$N$_3$O$_4$ in 75% yield.
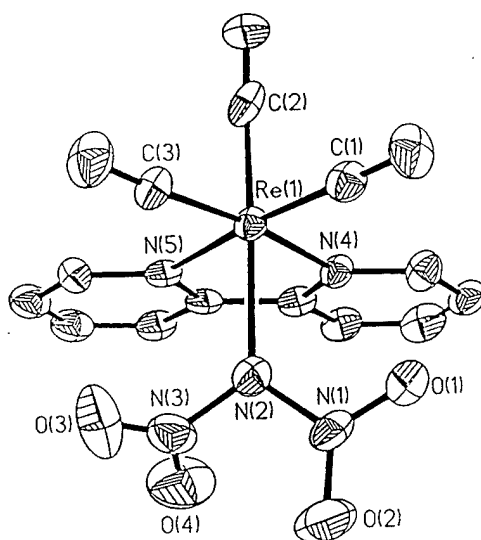
Figure 6. Crystal structure of *fac*-Re(bpy)(CO)3N3O4

The X-ray crystal structure presented in Figure 6 clearly shows that coordination occurs at the central nitrogen of the dinitramide ligand with the rest of the complex possessing the typical facial geometry exhibited by *fac*-Re(bpy)(CO)$_3$X complexes.

16

The Re-N bond lengths for the bpy ligand are 2.166 (10) Å (Re(1)-N(4)), and 2.160 (10) Å (Re(1)-N(5)). The Re-bpy bond lengths are typical of those in similar complexes of the type *fac*-Re(bpy)(CO)$_3$X (for X=OSO$_2$CF$_3$ [43] and PO$_2$F$_2$ [44] bond lengths are between 2.140 and 2.150 Å). The Re-N$_3$O$_4$ (Re(1)-N(2)) bond length is considerably longer, 2.223 (10) Å, consistent with its being a weaker donor than pyridine type ligands.

A structurally interesting feature is the "tilting" of the planar nitro groups away from each other along the Re(1)-N(2) axis where presumably because the oxygen atoms in close proximity are trying to increase their separation by rotating away from each other. The torsion angles (the twist of the NO$_2$ groups from the NNN plane) are significantly different compared to the free dinitramide ion (compare 11.2°, 59.6° to 22.6°, 19.9°). The central N atom in the dinitramide ligand is near planar, which stands in contrast to the calculated pyramidal structure of dinitraminic acid (the plane containing the Re-N bond is slightly bent from the NNN plane by 14°, whereas the latter compound has the plane containing the H-N bond predicted to be bent from the NNN plane by 60°).

3.3. Infrared Spectroscopic Studies Although vibrational assignments for coordinated dinitramide in *fac*-Re(bpy)(CO)$_3$N$_3$O$_4$ are made difficult due to the bipyridine ligand, comparison with the IR data of *fac*-Re(bpy)(CO)$_3$Cl allows identification of the bipyridine modes. In addition, we have prepared several other DN complexes for comparison, Re(CO)$_5$N$_3$O$_4$ and mer-Re(CO)$_3$(PPh$_3$)$_2$N$_3$O$_4$.

With these comparators, trends in the vibrational spectra of free versus coordinated N$_3$O$_4^-$ can be identified. The two striking changes that can be seen are the shift of the asymmetric NO$_2$ modes to higher energies by > 30 cm^{-1} and the loss of intensity for the N$_3$ asymmetric mode. These changes in the vibrational spectrum are apparently characteristic of a covalent central N-bonded structure, and should be useful for future comparisons.

3.4. Bonding Properties. As for all ligands, the Re-dinitramide interaction can be described in terms of σ donor, π donor or π acceptor ability. The degree to which each participates in the bond can be investigated by comparing properties of several Re carbonyl complexes with

17

varying X ligands. For example, the nature of the Re-X bond will manifest itself in the corresponding CO frequencies, bond lengths and Re-X substitutional lability. Thus, carbonyl stretching frequencies provide a measure of the electron density on the Re due to the ability of the $d\pi$ orbitals of the metal to back bond into the π^* orbitals of the CO's. These values are controlled by the nature of the X ligand, and it is clear that a good donor like Cl^- results in CO frequencies that are low compared to a weak donor like $SO_3CF_3^-$. In order to assay the bonding properties of dinitramide the simple force field model developed by Cotton and Kraihanzel[45] was used. In the CO stretching modes can be treated separately since they are high in energy and couple weakly with other vibrations. The coupling of vibrations between adjacent CO's is simplified by setting the interaction constants equal. The model has been successfully used to compare CO force constants of metal carbonyl complexes having similar structures.[46] In order to successfully the C-K mode, the correct IR spectral assignments must be made, fortunately ^{13}C isotopic labeling studies for fac-$Re(^{13}CO)_3(4,4'bpy)_2Cl$ clearly indicate that order of the observed CO frequencies is a' > a" > a'.[47]

The force constants of the CO trans to X (k_{ax}) vary significantly in the different complexes. For example, Cl^- being a good donor and a poor π acceptor has the smallest k_{ax} in the series. On the other hand, NO_2^- being a known π acid, has the largest. In other words, NO_2^- competes the most effectively with the trans CO for $d\pi$ density in the series of complexes. Likewise, by comparing k_{ax} of the Re complexes where X is $SO_3CF_3^-$ and N_3O_4 (considering both are poor donor ligands) demonstrates that $N_3O_4^-$ can π back-bond since k_{ax} for $SO_3CF_3^-$ is significantly smaller than for $N_3O_4^-$.

The strength of the Re-X bond can be indirectly related to its substitution lability if the mechanism of substitution is sensitive to bond breaking, for example a dissociative (D) or a dissociative interchange mechanism (I_d). The liabilities of a single ligand in different octahedral complexes have most commonly been investigated by solvolysis in aqueous solutions. Pentaamine complexes of $Co(III)(NH_3)_5X^{2+}$ have been studied extensively.[48] These solvolysis reactions often take place with the I_d mechanism, and likewise, the rates are very sensitive to the nature of

18

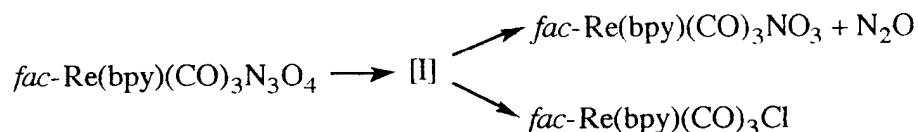the leaving groups and often parallel their basicity where stronger bases make poor leaving groups. For example, $t_{1/2}$ for the $Co(III)(NH_3)_5OSO_3CF_3^{2+}$ complex in water is 25 s, for $Co(III)(NH_3)_5NO_3^{2+}$, 8.0 hrs and $Co(III)(NH_3)_5Cl^{2+}$, 107 hrs.[49] The Re complexes seem to follow a similar trend for their solvolysis reactions in CH_3CN, however, it should be noted that the I_d mechanism has not been proven for the Re complexes. All of these experimental finding point to dinitramide as a poor *sigma* donor and a weak *pi* acceptor ligand.

3.5. Photochemistry of a coordinated $N_3O_4^-$.

fac-$Re(bpy)(CO)_3N_3O_4$ was found to be extremely photosensitive in solution. This is demonstrated by changes in the UV-Visible spectrum in CH_2Cl_2 (2.57 10^{-5} M) after irradiation (436 nm, 1000 W Hg lamp in a one cm cuvette) since the formation of a new product is seen. Analysis of the spectral changes (436 nm irradiation; monitoring the spectrum between 230 and 550 nm) is best approximated as an A $\rightarrow$ B $\rightarrow$ C process. Preparative photolysis in CH_2Cl_2 allows the isolation and characterization of C, which is identified as the nitrato complex *fac*-$Re(bpy)(CO)_3NO_3$ by comparison of its spectral properties to an authentic sample. For example, both the nitrato complex and the photolysis product have the same IR absorptions characteristic of a coordinated NO_3^{-}[50] (IR (ATR Cell) (v (ONO_2) cm^{-1}) 1475.7 N-O v_{as}, 1279.8, N-O v_s, 1001.5 v_2). NMR spectral shifts also compare well (*fac*-$Re(bpy)(CO)_3NO_3$: ^{1}H NMR (δ/ppm, CD_2Cl_2) 9.023 (d, 2H), 8.168 (m, 2H), 8.087 (m, 2H), 7.546 (m, 2H), the photolysis product: 9.023 (d, 2H), 8.167 (m, 2H), 8.088 (m, 2H), 7.54 (m, 2H)).

A minor product was also observed which tentatively has been assigned as the chloro complex *fac*-$Re(bpy)(CO)_3Cl$ by comparing the furthest downfield NMR resonance of *fac*-$Re(bpy)(CO)_3Cl$ (^{1}H NMR (δ/ppm, CD_2Cl_2) 8.96 (d, 2H) to the minor product (^{1}H NMR (δ/ppm, CD_2Cl_2) 8.95 (d)). The minor product could also be a nitro, *fac*-$Re(bpy)(CO)_3NO_2$, or a nitrito, *fac*-$Re(bpy)(CO)_3ONO$, complex, however, no characteristic IR absorbtions were found (v (ONO) cm^{-1}) : 1424 N-O, v_{as}, 1057 N-O v_s, (v (NO_2) cm^{-1}) 1372 N-O v_{as}, 1311 N-O v_s).

The stoichiometry of the photolysis reaction was determined by IR and NMR spectroscopic studies of the course of the reaction . After complete consumption of *fac*-$Re(bpy)(CO)_3N_3O_4$, the

product distribution (with respect to the metal) was 90% *fac*-Re(bpy)(CO)$_3$NO$_3$. N$_2$O was also produced, which is consistent with the reaction written below.

$$\textit{fac-}\text{Re(bpy)(CO)}_3\text{N}_3\text{O}_4 \longrightarrow \text{[I]} \Bigg\langle \begin{array}{l} \textit{fac-}\text{Re(bpy)(CO)}_3\text{NO}_3 + \text{N}_2\text{O} \\[2ex] \textit{fac-}\text{Re(bpy)(CO)}_3\text{Cl} \end{array}$$

This photoreaction is extraordinary. Since irradiation at 436 nm predominantly populates Re(I) to bpy MLCT excited states to the exclusion of dinitramide states it is apparently a rare example[4] of intramolecular chemistry photosensitized by a MLCT excited state. This is made more intriguing by the fact that the quantum yield (ϕ_{436}) is very high (0.67±0.05 in air and 0.97±0.05 under N$_2$). Special care for the calculation of the quantum yield had to be taken since the intermediate and products of the photolysis also absorb the incident radiation.

From the action spectrum, the quantum yield for the decomposition of Re(bpy)(CO)$_3$N$_3$O$_4$ is independent of wavelength . The action spectrum is the rate of photolysis (k_l) plotted against the excitation wavelength. Since both the action spectrum and absorption spectrum overlay each other, it is apparent that the lowest MLCT state is responsible for the decomposition of the dinitramide ligand.

By lowering the triplet energy of the MLCT excited chromophore, the quantum yield at 436 nm is dramatically reduced. For example, *fac*-(4,4'-NO$_2$bpy)Re(CO)$_3$N$_3$O$_4$, which exhibits a dramatically red-shifted MLCT transition has a quantum yield of 0.003 (436 nm excitation, air saturated). However, excitation at 366 nm increases the quantum yield to 0.5 which suggests that excitation at 366 nm for this complex directly populates the dinitramide state responsible for its decomposition.

3.6. Sensitized Photochemistry of the Dinitramide Ion. As demonstrated in in the work above, energy transfer from a MLCT excited state to a ligand localized N$_3$O$_4^-$ state is apparently involved in the photochemistry of the coordinated N$_3$O$_4^-$ in *fac*-Re(bpy)(CO$_3$)N$_3$O$_4$. To further address the issue of energy versus electron transfer to dinitramide, we have studied

20

intermolecular sensitization photochemistry. Transition metal complexes with metal to ligand charge transfer (MLCT) excited states are well known probes for the investigation of nuclear and electronic factors involved in photoinduced electron and energy transfer processes. As mentioned later in this report, the ease of reduction of $N_3O_4^-$ makes it a candidate as an oxidative quencher of molecular excited states. Since MLCT excited states of $Ru(LL)_3^{2+}$ complexes originate from the promotion of an electron from a primarily $d\pi$ orbital to a π^* orbital of a diimine ligand (LL), the excited state properties of these chromophores can be "tuned" simply by changing the diimine ligands. In addition, $Ru(LL)_3^{2+}$ excited states have sufficiently long lived lifetimes and should be able to undergo electron or energy transfer bimolecular reactions in solution as shown in the eqs below. By changing the substituents on the diimine aromatic ring system, the $d\pi$ and π^* levels can be shifted to favor energy or electron transfer and thus can be used as a diagnostic tool for mechanism determination. The majority of the detailed results can be found in the second and third year reports.

Strong evidence for photoinduced electron transfer has been shown with the Marcus analysis of quenching studies of $Ru(LL)_3^{2+}$ excited states by the dinitramide ion. In addition, the fact that the steady state photolysis of the dinitramide ion in water by $Ru(LL)_3^{2+}$ excited states can be driven with addition of a reductive scavenger also supports an electron transfer mechanism. Also, attempts to sensitize the dinitramide ion with methylene blue (the triplet energy of methylene blue is 1.4 eV) showed no decomposition which is consistent with $Ru(TAP)_3^{2+}$ quenching results where there was no observed energy transfer at 2.1 eV. In conclusion, by taking into account electrostatic considerations and driving force, the irreversible photosensitized reduction of the dinitramide anion can be driven by the choice of the sensitizer and ionic strength of the medium. This is of obvious imterest if enviromentally-reactive senstizers (like humic excited states) are in proximity to a steady state concentration of DN (from transport).

3.7. Electrochemical Studies of Dinitramide. Dinitramide redox chemistry has been studied at several pH values. Figure 7 shows the cyclic voltammogram (CV) for KDN (the potassium salt of dinitramide) at a pH of 6.36. This experiment clearly reveals two separate, 2

electron reduction processes at potentials of ca. -0.30 V and -0.82 V vs Ag/AgCl, respectively. These reduction processes are chemically irreversible, meaning that the direct products of the reductions disappear extremely rapidly. These results further show that both of these processes produce nitrite as a product of the reduction. The presence of nitrite is revealed by virtue of the oxidation wave at ca. +0.83 V (i.e. the oxidation process is observed as a prewave before the gold oxidation). Control experiments in which nitrite was purposefully added to the cell have verified that this wave is, indeed, due to nitrite oxidation. Its position as a prewave of the gold oxide formation wave suggests the catalysis of this oxidation process by the oxide, a mechanism that would be consistent with previous findings in regards to anodic oxygen transfer catalysis at oxide electrodes.[51] Thus, at a pH of 6.36 DN is first reduced in a two electron step at ca. -0.30 V to produce nitrite plus a product (which we believe to be nitraminic acid) that is itself reducible in a two electron process, where this second reduction also produces nitrite. The product of the second reduction process is uncertain at this time, although it seems likely that it is ammonium ion (see below).

Figure 8 shows the scan rate dependence of the two reduction waves for DN at a pH of 6.36. The peak currents for these waves are plotted in Figure 9 versus the square root of scan rate. These plots demonstrate that these reduction waves are characteristic of the delivery of DN to the electrode surface via diffusion, as expected. In addition, the deviation from linearity of the plots at higher scan rates is suggestive of kinetic limitations for the transfer of electrons between the electrode surface and the compound near the surface (after it has diffused to the surface). In other words, the heterogeneous electron transfer kinetics for DN appear to be relatively slow, or, in the terminology of electrochemistry, the reduction process is electrochemically irreversible. Further, it should be noted that these two waves are observable only after repeated scanning over the gold oxide waves, a procedure that is well known to clean the Au surface of contaminants. Additionally, the ability to observe these waves on other electrode materials (including Cu, Ag, Pt, and C) is similarly influenced by the state of cleanliness of the electrode surface. Specifically, electrode surfaces that are not scrupulously clean do not show these reduction processes. It is also

interesting that no waves are evident on glassy carbon electrodes. This strong dependence of the ability to observe the redox processes for DN on the state of cleanliness of the electrode surface is consistent with the observation of relatively slow heterogeneous electron transfer kinetics. The dependence on electrode material suggests that adsorption is a key step in the electrochemical reduction process.

Figure 10 shows the results of CV experiments similar to those presented in Figures 7 and 8 above, but at a pH of 2.26. In this case, the reduction of DN via a two electron process is still observed, this time at a potential of ca. -0.10 V. Thus, the potential for the first redox process is shifted with respect to its position at a pH of 6.36, a point to which we will return below. This CV also shows a second wave at ca. -0.8 V. However, this wave is also present in the background and is due to reduction of protons to produce hydrogen. We believe the second wave for DN is present under this background process, but is obscured by the larger currents due to proton reduction and the relative proximity of these two reduction processes. Recently, experiments were done at a variety of pH values between 6.36 and 3.5, using phosphate buffers to control the pH. These experiments clearly reveal the presence of both reduction processes for DN at all pH values from 6.36 to 3.5, lending credence to this interpretation of the data at pH = 2.2.

Figure 7.
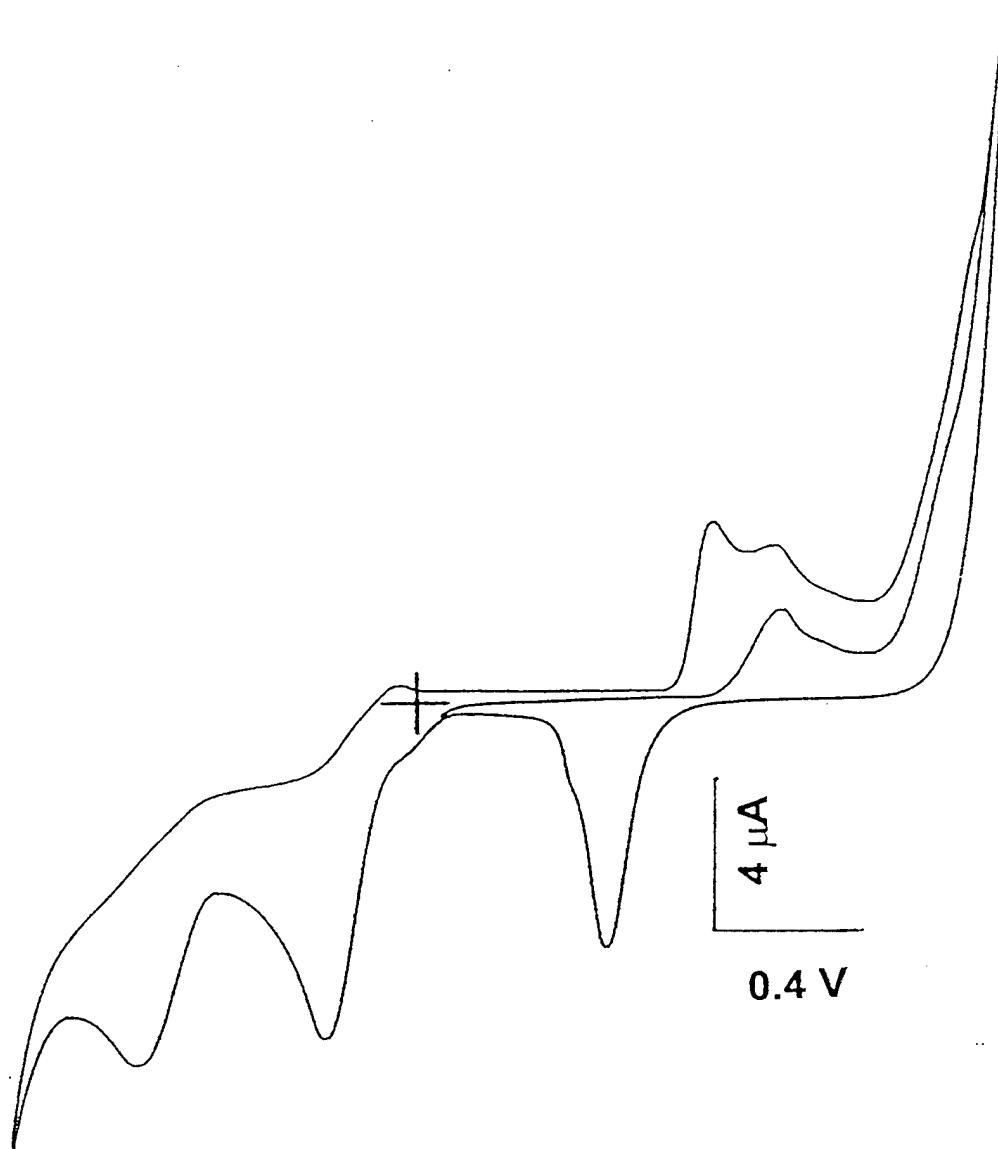
CV of 2 mM dinitramide in 0.1 M NaNO$_3$ with 10 mM phosphate buffer at pH = 6.4, limits - 1.1 to 1.6 V vs Ag/AgCl, v = 50 mV/s.
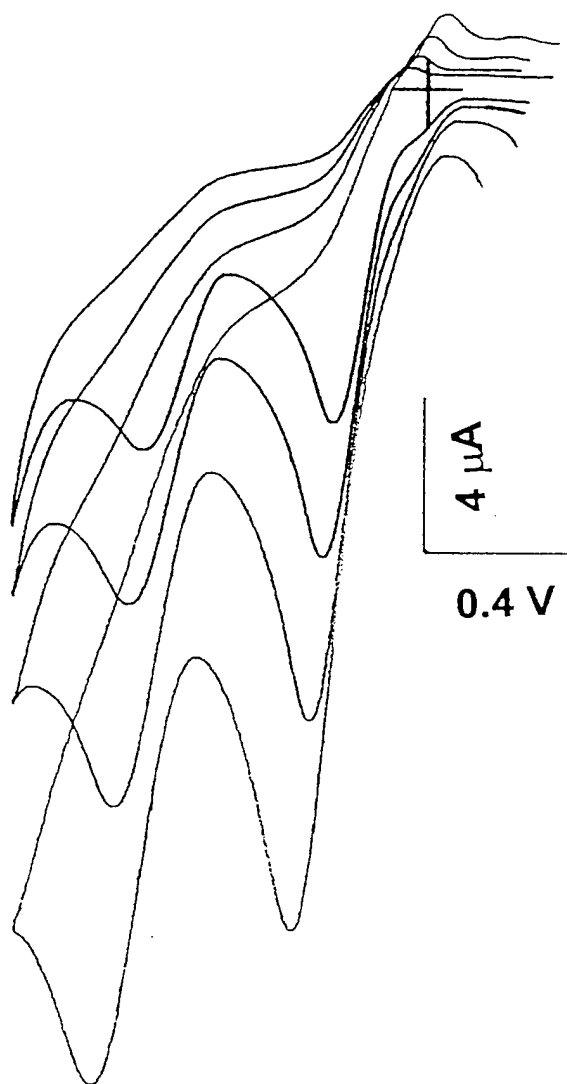
Figure 8.

CV of 2 mM dinitramide in 0.1 M NaNO$_3$ with 10 mM phosphate buffer at pH = 6.4, limits - 1.1 to ca. 0.35 V vs Ag/AgCl, ν = 50, 100, 200, 400 mV/s.
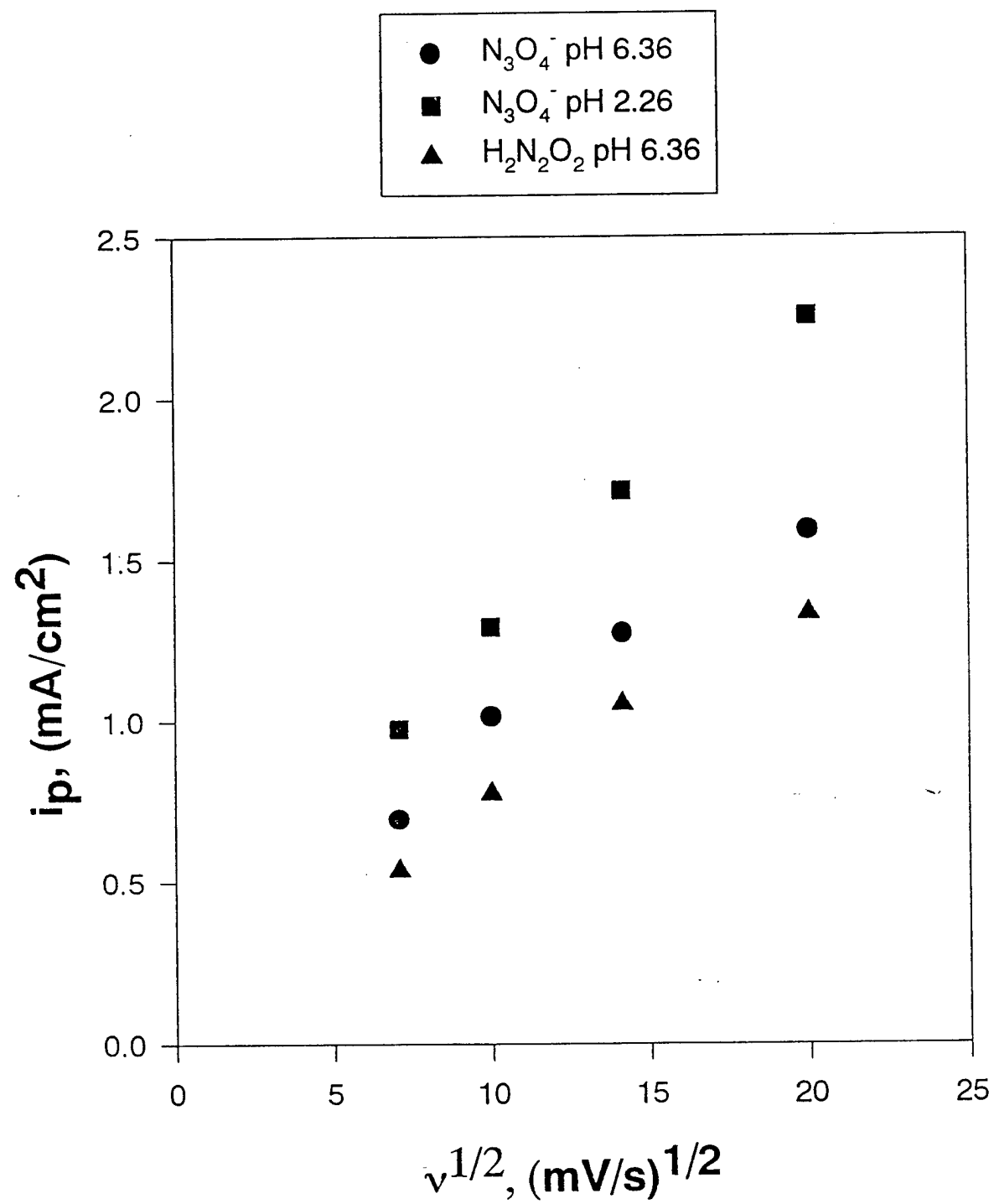
Figure 9.

Legend:
- ● $N_3O_4^-$ pH 6.36
- ■ $N_3O_4^-$ pH 2.26
- ▲ $H_2N_2O_2$ pH 6.36

Y-axis: i_p, (mA/cm^2)
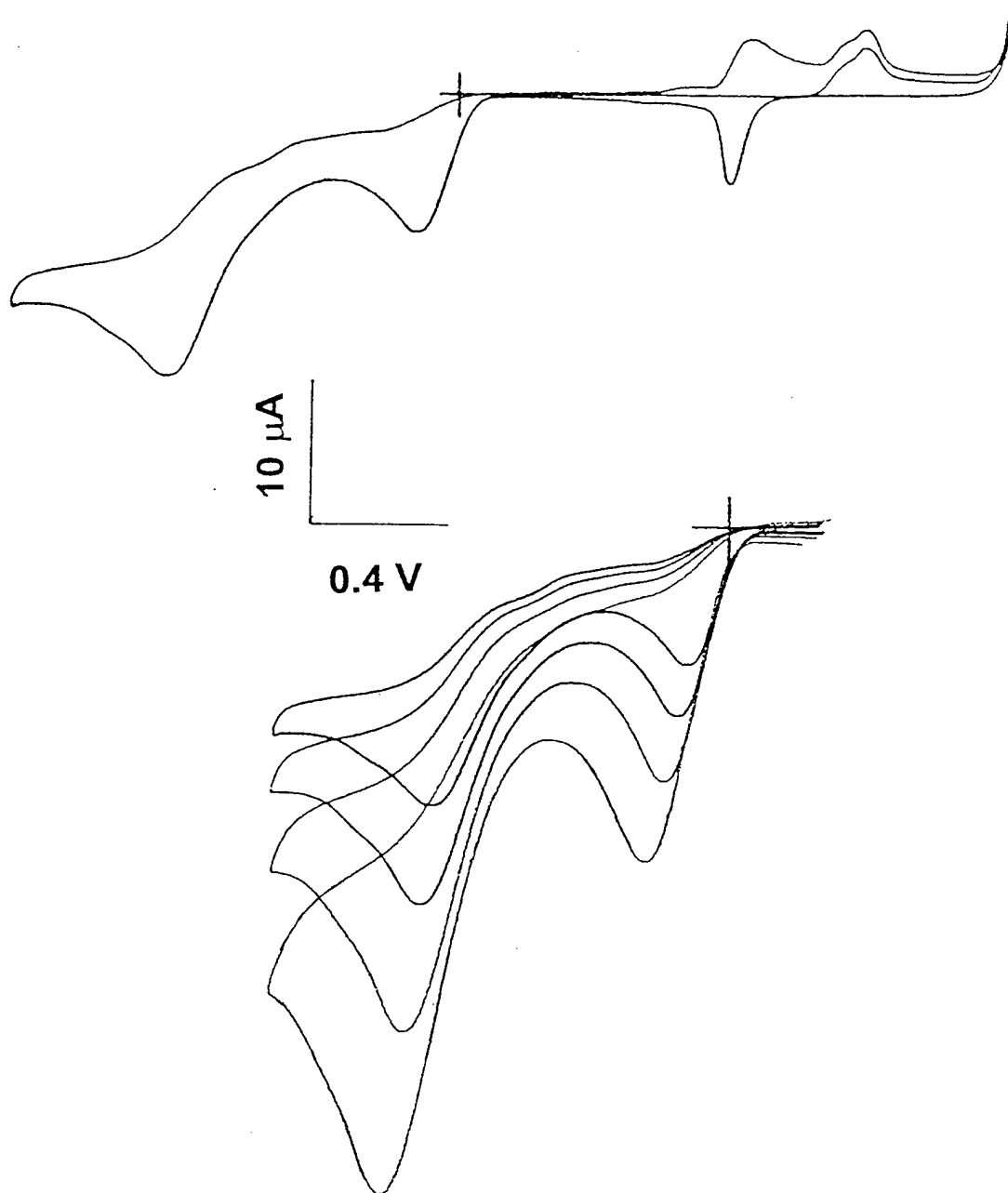
X-axis: $\nu^{1/2}$, $(mV/s)^{1/2}$

Figure 10.

Top: CV of 2 mM dinitramide in 0.1 M NaNO$_3$ at pH 2.2, v = 50 mV/s, limits -1.3 V to 1.6 V vs Ag/AgCl.

Bottom: CV of 2 mM dinitramide in 0.1 M NaNO$_3$ at pH 2.2, limits -1.3 V to 1.6 V vs Ag/AgCl, v = 50, 100, 200, 400 mV/s.
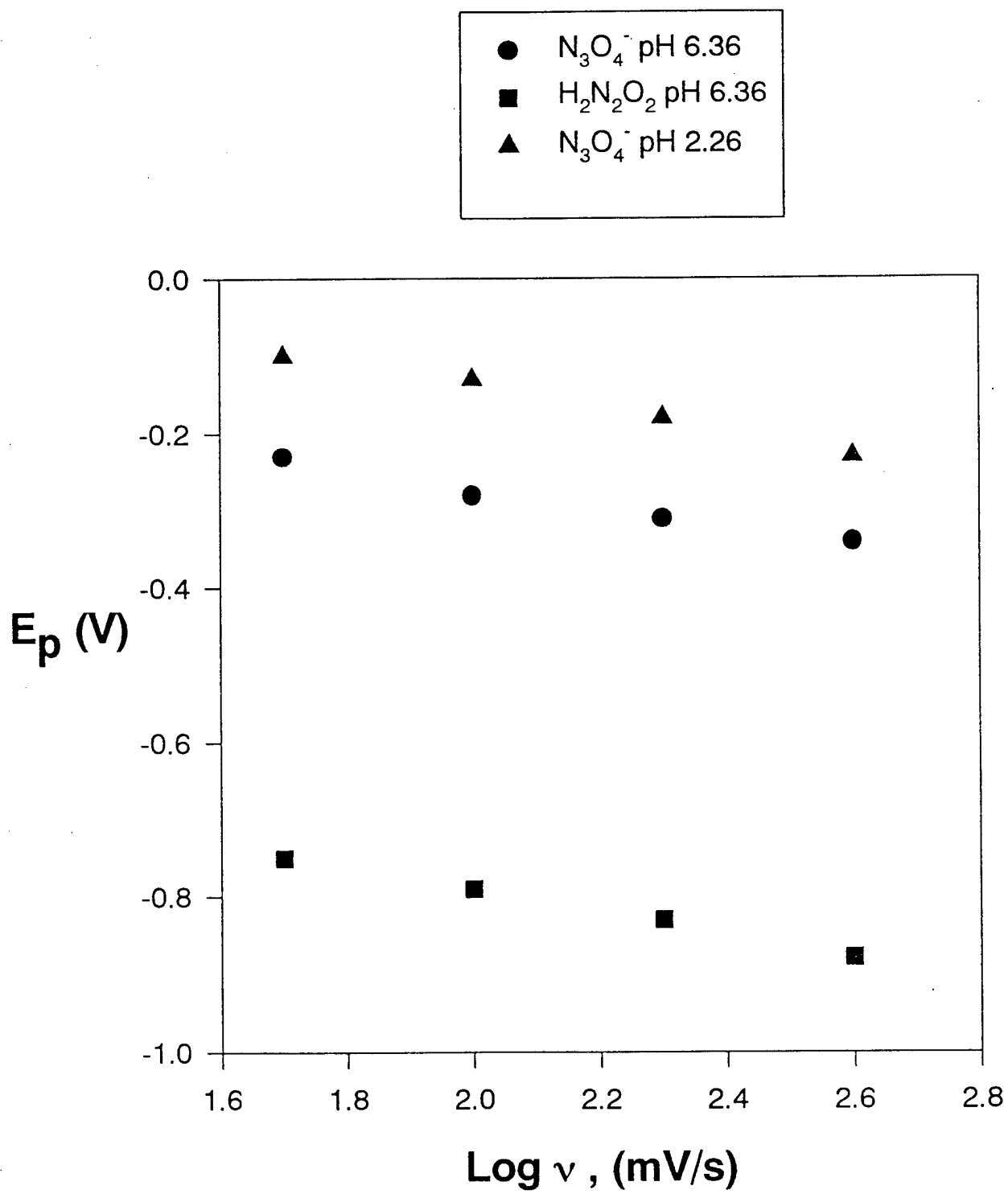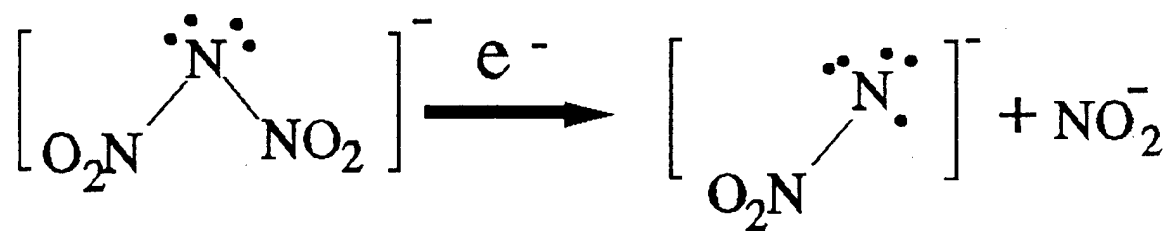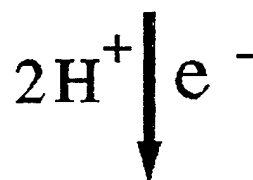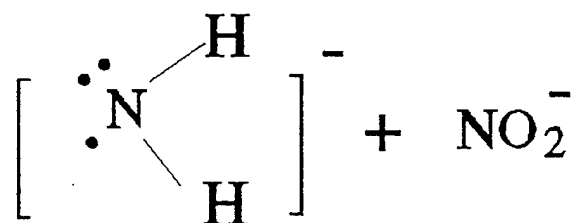
Figure 11.

Legend:
- ● $N_3O_4^-$ pH 6.36
- ■ $H_2N_2O_2$ pH 6.36
- ▲ $N_3O_4^-$ pH 2.26

Y-axis: E_p (V)

X-axis: Log ν, (mV/s)

Figure 12.

$$\left[\begin{array}{c} \ddot{N} \\ O_2N \quad NO_2 \end{array} \right]^- \xrightarrow{e^-} \left[\begin{array}{c} \ddot{N} \\ O_2N \end{array} \right]^- + NO_2^-$$

Dinitramide

$$\Big\downarrow 2H^+ \Big| e^-$$

$$H^+ + HN\text{-}NO_2^- \rightleftharpoons H_2N\text{-}NO_2$$

Nitraminic Acid

$$\Big\downarrow e^-$$

$$\left[\begin{array}{c} \ddot{N} \quad H \\ \quad H \end{array} \right]^- + NO_2^-$$

$$\Big\downarrow 2H^+ \Big| e^-$$

$$NH_4^+$$
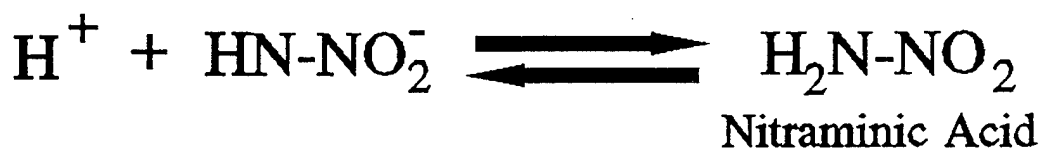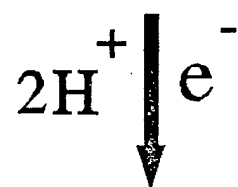
The upper CV in Figure 10 also clearly shows the production of nitrite as a consequence of the DN reduction process, as evidenced by the oxidation wave at 0.84 V, again as a prewave of the gold oxide wave. In a separate set of experiments, it was determined that the magnitude of this nitrite oxidation wave depends on whether the first or second DN reduction process has been traversed. The fact that the nitrite wave approximately doubles after passing over the second reduction wave, with respect to its magnitude after passing over the first wave (not shown), comprises the evidence that the second reduction of DN is actually present under the proton reduction wave. The lower set of CV's in Figure 10 show the scan rate dependence of the responses. These are plotted versus the square root of scan rate in Figure 9, once again verifying the origin of the wave as due to a diffusion process and demonstrating slow heterogeneous electron transfer kinetics. An additional feature of the this set of CV's is the relative independence of the rising part of the first reduction wave on scan rate. This feature has been qualitatively attributed to slow heterogeneous electron transfer kinetics (2), an assignment that would be in agreement with the curvature observed in the plots in Figure 9 and the observations as to the dependence of the redox process on the state of the electrode surface.

Figure 11 shows plots of the peak potential, E_p, for the reduction processes observed at pH values of 6.36 and 2.26 versus the logarithm of scan rate. (Note that the E_p for the second wave is not plotted at the lower pH value because it is obscured by the proton reduction wave.) These plots clearly show the pH dependence of the first reduction process as well as the dependence of the E_p on scan rate. The relatively large slopes of these plots (ca. 100 - 160 mV/decade change in scan rate) are not consistent with fast heterogeneous electron transfer kinetics.[52] Rather, they are consistent with the interpretation given above that the electron transfer is electrochemically irreversible. However, the observation of pH dependent peak positions suggests that the peak shape and position are a convolution of the influence of slow electron transfer kinetics and a fast follow-up reaction involving protonation. We return to this point below in the discussion of a mechanism for these reduction processes.

Figure 12 shows a proposed mechanism that is consistent with the observations reported above. The first step involves what is probably a concerted electron transfer/bond cleavage event that produces nitrite and a radical species. This electron transfer is likely to be the rate-limiting step in the overall process. The dissociation of the N-N bond is responsible for the chemical irreversibility of this first reduction process. The radical will then be reduced and protonated in a rapid follow-up process(es) to give nitraminic acid. The question of whether one or two protons are transferred to this product depends on the pH, since the pKa of nitraminic acid is 6.56 (i.e. two protons will be transferred at pH values below 6.56). It seems reasonable that only one electron would be transferred during this follow-up chemistry, both because this is consistent with observation of an overall two electron process for the first wave, and because the nitraminic acid product is likely to be relatively stable under these conditions. We further propose that the second, two electron reduction process proceeds in a manner analogous to the first. Thus, a concerted electron transfer/bond cleavage event occurs, producing both nitrite and a radical product that is reduced further and protonated in rapid follow-up chemistry. We believe it is the protonation process(es) associated with this rapid follow-up chemistry that lead to the pH dependence of the E_p's, a speculation that is consistent with the experimental observations.

The picture that emerges from these electrochemical studies is one in which each molecule of DN undergoes two separate, kinetically complicated, two electron reduction processes to produce two molecules of nitrite plus one molecule of ammonium. These results and their interpretation are the subject of a manuscript that is under preparation.[53]

3.5 Microbiological Results on DN.

Our biological results indicated that DN is not used by aerobic bacteria as a sole N source (experiments involved both pure cultures of the genus *Pseudomonas* and aerobic soil microcosms) and is apparently not toxic. Recently, similar results were obtained with pure cultures of anaerobic bacteria (i.e., *Pseudomonas dentrificans* grown under nitrate-reducing conditions and the sulfate-reducing bacteria *Desulfovibrio desulfuricans*).

In contrast, *P. aeruginosa* is able to catalyze transformation of DN under aerobic conditions, but only when NH_4^+ is present as the N source (30 mM). The products of DN transformation apparently are NH_4^+ and NO_2^- as is suggested by their increased concentrations in cultures grown in the presence of DN. It is interesting to note that nitrite formation is consistent with a reductive mechanism as first indicated by our electrochemical studies. Preliminary evidence using cell-free systems suggests that this DN transformation is either an intracellular or membrane-bound process; however the role of NH_4^+ in DN transformation is currently unknown.

Biodegradation of dinitramide (DN) has been studied under anaerobic conditions. A sulfate-reducing consortium enriched from a lake sediment was obtained and DN was degraded by this consortium when lactate was the energy source. DN was depleted when served either as a nitrogen source or a potential electron acceptor for the consortium. DN disappearing in the media co-occurs with the tentative termination of sulfate reduction. No obvious intermediates were detected during the DN depletion.

4. References

1) Bryusova, L. *J. Gen Chem. U.S.S.R.*, **1936**, *6*, 667.

2) Hautala, R.R., King, R.B., Kutal, C. "Solar Energy: Chemical Conversion and Storage" Hautala, R.R., King, R.B., Kutal, C.: editors; Humanna Press, Clifton, NJ, pp. 333-69.

3) Miki, S; Asako, Y; Yoshida, Z. *Chem. Lett.* **1987**, 195.

4) Alberici, F; Cassar, L; Monti, F; Neri, C; Nodari, N., Eup. Pattent 420325 A1 910403. "High Energy Fuel Composition Containing Quadricyclane."

5) Gassman P.G.; Yamaguchi, R.; Koser, G.F. *J. Org. Chem.* **1978**, *43*, 4393.

6) Yasufuku, K.; Takahashi, K. *Tet. Lett.* **1984,** *25*, 4893.

7) Chen, G.: Tzong, W.; Williams, F. *J. Am. Chem. Soc.* **1991,** *113*, 9853.

8) Cromack, K.R.; Werst, D.W.; Barnabas, M.V.; Trifunac, A.D. *Chem. Phys. Lett.* **1994,** *218*, 485.

9) Ford, J.F.; Mann, C.K.; Vickers, T.J. *Appl. Spec.* **1994,** *48*, 592.

10) Hill, W.E.; Szechi, J.; Hofstee, C.; Dane, J.H. *Environ. Sci. Technol.* 1997, *31*, 651.

11) Tabushi, I; Yamamura, K., *Tetrahedron,* **1975**, *31*, 1827.

12) Weng H, Roth H.D. *J. Org. Chem.* **1995**, *60*, 4136.

13) Koser G. F., Faircloth J. N. *J. Org. Chem.* **1976**, *41*, 583.

14) Yasfuku, K.; Takahashi, K., Kutal, C. *Tet. Lett. 1984*, **25**, 4893.

15) Bach, R.D.; Schilke, I.L.; Schlegel, H.B., *J. Org. Chem.* **1996**, *61*, 4845.

16) Sullivan, B.P.; Dickey, M.; Seward, K., Manuscript in preparation

17) Buttry, D.A., White, K.C., Manuscript in preparation

18) Wiberg, K.B.; Cuila, R.P. *J. Am. Chem. Soc.* **1959**, *81*, 5216.

19) Gassman, P.G.; Yamaguchi, R.; Koser, G.F. *J. Org. Chem.* **1978**, *43*, 4392.

20) Shono, T.; Matsumura, K. *J. Org. Chem.* **1970**, *35*, 4157.

21) Gassman, P.G.; Hershberger, J.W. *J. Org. Chem.* **1987**, *52*, 1337.

22) Wright, J. *J. Am. Chem. Soc.* **1993**, *58*, 4122.

23) Bard, A.J., Faulkner, L.R., "Electrochemical Methods Fundamentals and Applications"John Wiley & Sons, Inc. 1980.

24) Mirabella, F.M. Jr., History of Internal Reflection Spectroscopy, "Internal Reflection Spectroscopy" Mirabella, F.M. Jr. Editor.

25) Atlas, R.M. *Microbiol. Rev.* **1981**, *45*, 180-209.

26) Chiang, C.Y., J.P. Salanitro, E.Y. Chai, J.D. Colthart, and C.L. Klein *Ground Water* **1989**, *27*, 823.

27) Herbes, S.E. and L.R. Schwall *Appl. Environ. Microbiol.* **1978**, *35*, 306.

28) MacMillan, D.K., R.N. Hayes, D.A. Peake and M.L. Gross *J. Am. Chem. Soc.* **1992**, *114*, 7801.

29) Kirkor, E.S., V.M. Maloney and J. Michl. *J. Am. Chem. Soc.* **1990**, *112*, 148.

30) Ristic, G.S., M.D. Marinkovic, J.J. Comor, V.M. Vasic, M.S. Ristic and R.M. Nikolic. *J. Mol. Struct.* **1992**, *267*, 7.

31) Leahy, J.G. and R.R. Colwell.*Appl. Environ. Microbiol.* **1990**, *54*, 305.

32)   Perry, J.J. In: R.M. Atlas, ed., *Petroleum Microbiology*. Macmillan Publishing Co., New York, NY, pp. 61-98, 1988.

33)   Redfern, P.; Politzer, P. "Computational Analyses of Structural Properties of the Dinitramide Ion, $N_3O_4^-$ and Related Molecules: Dinitramine and Trinitroamine", ONR Technical Report AD -A228 139, 1990.

34)   Politzer, P.; Seminario, J. M.; Concha, M. C.; Redfern, P. C. *J. Mol. Structure (Theochem)* **1993**, *287*, 235-240.

35)   Michels, H. H.; Montgomery, J. A. J. *J. Phys. Chem.* **1993**, *97*, 6602-6606.

36)   Schmitt, R. J.; Krempp, M.; Bierbaum, V. M. *Int. J. Mass Spectrom. Ion Processes* **1992**, *117*, 621.

37)   Luk'yanov, O. A.; Gorelik, V. P.; Tartakovsky, V. A. *Russ. Chem. Bull.* **1994**, *43*, 89.

38)   Bottaro, J. C.; Schmitt, R. J.; Penwell, P. E.; Ross, D. S. U.S. Patent 5,254,324, Oct. 19, 1993.

39)   Christe, K. O.; Wilson, W. W.; Petrie, M. A.; Michels, H. H.; Bottaro, J. C.; Gilardi, R. *Inorg. Chem.* **1996**, *35*, 5068-5071.

40)   Personal communication with Dr. Richard Gilardi at the Naval Research Laboratory, Washington, D.C., 1996.

41)   Shlyapochnikov, V. A.; Oleneva, G. I.; Cherskaya, N. O.; Luk'yanov, O. A.; Gorelik, V. P.; Anikin, O. V.; Tartakovsky, V. A. *Russ. Chem. Bull.* **1995**, *44*, 1449.

42)   Shlyapochnikov, V. A.; Cherskaya, N. O.; Luk'yanov, O. A.; Anikin, O. V.; Tartakovsky, V. A. *Russ. Chem. Bull.* **1996**, *45*, 430.

43)   Calabrese, J. C.; Tam, T. *Chem. Phys. Lett.* **1987**, *133*, 244.

44)   Horn, E.; Snow, M. R. *Aust. J. Chem.* **1980**, *33*, 2369.

45)   Cotton, F. A.; Kraihanzel, C. S. *J. Am. Chem. Soc.* **1962**, *84*, 4432.

46)   A suitable crystal for X-ray analysis was provided by Kevin Seward.

47) Gamelin, D. R.; George, M. W.; Glyn, P.; Grevels, F. W.; Johnson, F. P. A.; Klotzbucher, W.; Morrison, S. L.; Russell, G.; Schaffner, K.; Turner, J. J. *Inorg. Chem.* **1994**, *33*, 3246.

48) Wilkins, R. *Kinetics and Mechanism of Reactions of Transition Metal Complexes*; VCH Publishers: New York, 1991.

49) Taube, H.; Armor, J. N. *J. Am. Chem. Soc.* **1969**, *24*, 91.

50) See, for example, Larew, L.; Gordon, J.S.; Hsiao, Y.-L.; Johnson, D.C.; Buttry, D.A. *J. Electrochem. Soc.* **1990, 137,** 3071 and references therein.

51) Klingler, R.J.; Kochi, J.K. *J. Am. Chem. Soc.* **1980,** *102*, 4790.

52) Cox, R.; Seeley, K.; Sullivan, B. P.; Buttry, D. A. *J. Electrochem. Soc.*, in preparation.

Status of Publications (published, submitted or in preparation).

The following list are of papers being prepared, submitted or that are published concerning the project. These can be considered the minimum output from the original project.

Jin, S., N. G. Swoboda-Colberg and P. J. S. Colberg. "Persistence, Inhibition of Bacterial Growth and Acute Toxicity of Quadracyclane and its Transformation Product Tricyclic[2.2.1.02,6]heptan-3-ol." Manuscript submitted to Environ. Toxicol. Chem.

Jin, S., N. G. Swoboda-Colberg and P. J. S. Colberg. "Microbial Degradation Tricyclic[2.2.1.02,6]heptan-3-ol: a Major Transformation Product of Quadracyclane in Soil." Manuscript submitted to Can. J. Microbiol.

Jin, S., and P. J. S. Colberg. "Aerobic Cometabolism of Dinitramide by *Pseudomonas aeruginosa* with Ammonium as a Source of Nitrogen." Manuscript in preparation.

Trammell, S.; Goodson, P.A.; Sullivan, B.P., 1996, "Coordination Chemistry and Photoreactivity of the Dinitramide Ion," Inorg. Chem. 35, 1421.

O' Toole, T. R.; Meyer, T. J.; Trammell, S.; Sullivan, B. P. "Electrocatalytic Dehalogenation by Re-Based Radicals." submitted to Inorg. Chem.

Trammell, S.; Cox, R.; Buttry, D. A.; Sullivan, B. P. "Reversible and Irreversible Photosensitized Reduction of the Dintramide Anion." manuscript in preparation.

Cox, R.; Seeley, K.; Buttry, D. A. "Electrochemical Reduction of Dinitramide Ion in Aqueous Solution." manuscript in preparation.

White, K.; Buttry, D. A. "Electrochemical Oxidation of Quadracyclane in Aqueous Solution." manuscript in preparation

We also have awarded an M.S. degree based on this work: Kathy Tomlinson, 1995, "Highly Strained, Saturated Hydrocarbon Compounds: Exploring their Fundamental and Redox

Chemistries, Application for Energy Conversion and Storage, and Environmental. Impacts Using Quadracyclane as a Working Model"

Four Ph.D. dissertations are partially or totally devoted to this project. Also four abstracts concerning the work have been submitted to scientific meetings.